

## REPORT DOCUMENTATION PAGE

Form Approved  
OMB No. 0704-0188

1a. REPORT SECURITY CLASSIFICATION		1b. RESTRICTIVE MARKINGS	
2a. SECURITY CLASSIFICATION AUTHORITY		3. DISTRIBUTION / AVAILABILITY OF REPORT	
2b. DECLASSIFICATION / DOWNGRADING SCHEDULE		4. PERFORMING ORGANIZATION REPORT NUMBER(S)	
5. MONITORING ORGANIZATION REPORT NUMBER(S)		6a. NAME OF PERFORMING ORGANIZATION	
6b. OFFICE SYMBOL (If applicable)		7a. NAME OF MONITORING ORGANIZATION	
7b. ADDRESS (City, State, and ZIP Code)		8a. NAME OF FUNDING / SPONSORING ORGANIZATION	
8b. OFFICE SYMBOL (If applicable)		9. PROCUREMENT INSTRUMENT IDENTIFICATION NUMBER	
10. SOURCE OF FUNDING NUMBERS		11. TITLE (Include Security Classification)	
PROGRAM ELEMENT NO.		PROJECT NO.	
TASK NO.		WORK UNIT ACCESSION NO.	
12. PERSONAL AUTHOR(S)		13a. TYPE OF REPORT	
13b. TIME COVERED		14. DATE OF REPORT (Year, Month, Day)	
15. PAGE COUNT		16. SUPPLEMENTARY NOTATION	
17. COSATI CODES		18. SUBJECT TERMS (Continue on reverse if necessary and identify by block number)	
FIELD		GROUP	
SUB-GROUP		19. ABSTRACT (Continue on reverse if necessary and identify by block number)	
20. DISTRIBUTION / AVAILABILITY OF ABSTRACT		21. ABSTRACT SECURITY CLASSIFICATION	
22a. NAME OF RESPONSIBLE INDIVIDUAL		22b. TELEPHONE (Include Area Code)	
22c. OFFICE SYMBOL		22d. NAME OF RESPONSIBLE INDIVIDUAL	

## I. "MOTION COHERENCE"

### A. The Experimental Findings

To find evidence for the operations of a trajectory network, a small signal was embedded within a large field of random noise. The signal was a single dot, moving in apparent motion in a consistent direction, amidst identical noise dots in random apparent motion. Casco, Morgan and Ward (1989) had measured " $d_{\max}$ " for a single dot presented in the midst of dynamic visual noise, but in their study, the motion of the signal dot was quite different from that of the flickering noise dots<sup>1</sup>. In our paradigm, the spatial (step size) and temporal (frame rate) characteristics of the motion were the same for both the signal and noise dots. Thus, it was impossible to discriminate between the signal and noise dots on the basis of any pair of frames. Only the consistency of its direction distinguished the motion of the signal dot from that of the noise dots.

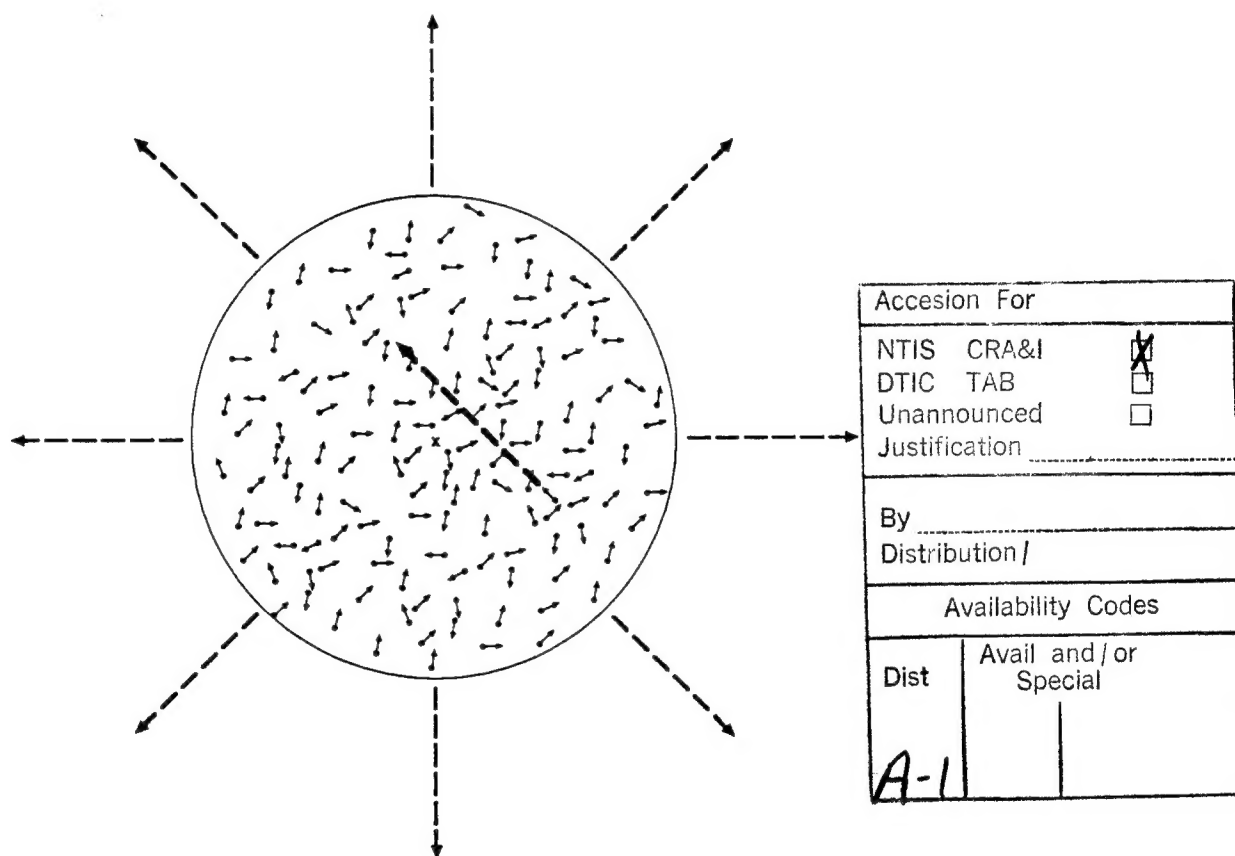


Figure 1

A schematic representation of the display is shown in Figure 1. The noise dots were presented within a 10 degree circular aperture. The signal dot moved in one of eight directions chosen at random, as indicated by dashed arrows drawn around perimeter of the circle in Figure 1. Observers were instructed to fixate the center of the aperture (shown by the x in the center). The middle of the trajectory was constrained to be within a 2-by-2 degree window centered on the

<sup>1</sup> " $D_{\max}$ " is the maximum displacement in a single jump (2 frames) in which the direction of the displacement can be reliably judged according to a standard threshold criterion.

fixation point, but the vertical and horizontal location of the trajectory was changed at random from trial-to-trial. Hence, it seldom passed directly under the fixation point. In a 2AFC paradigm, observers were shown two presentations, one containing only the noise dots and the other the noise plus the signal dot; they judged which of the two presentations contained the signal. Feedback was provided in all experiments

Our results led to three conclusions:

1) *Detection is limited by the probability of mismatch, not noise density.*

Detection was measured as a function of noise density with step size as a parameter. As shown in the upper half of Figure 2, the effect of noise density depended systematically on the step size. At large step sizes, even low density noise (0.5 dots/deg<sup>2</sup>) degraded detection, while at small

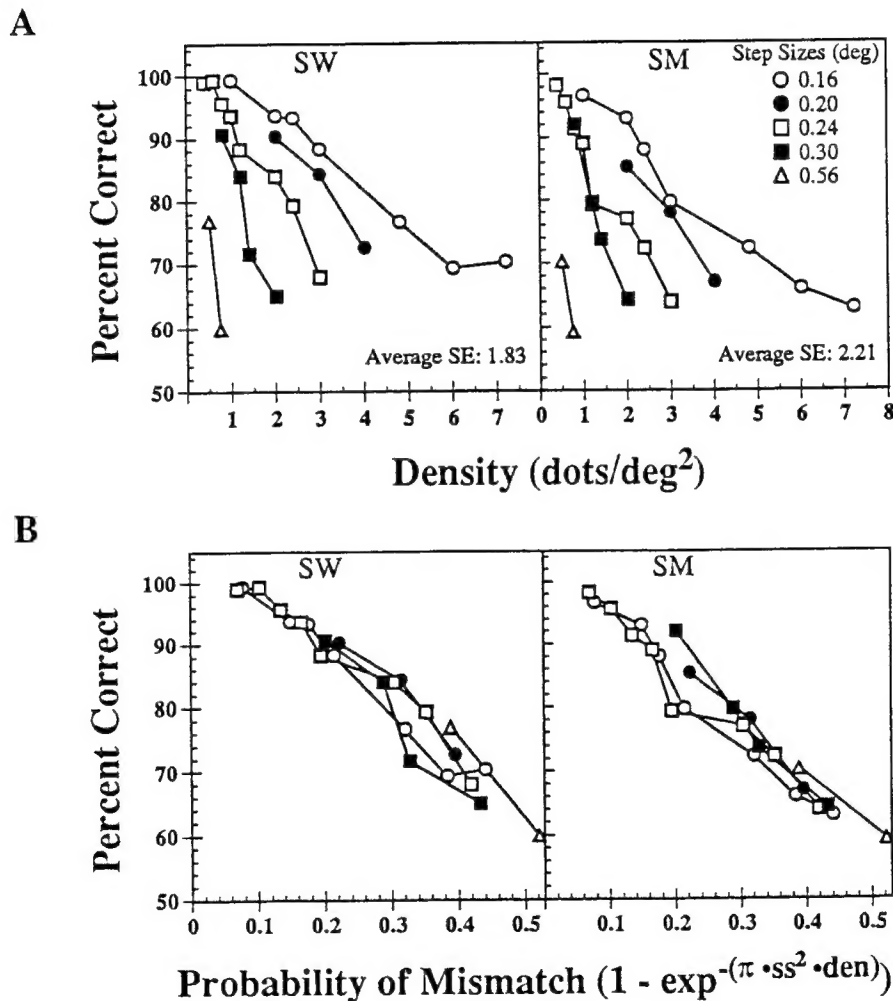


Figure 2

step size sizes, low density noise had almost no effect. Recall that both the signal and the noise dots were moving in apparent (sampled) motion. In the context of apparent motion, one quantity that depends jointly on step size and density is the probability of a mismatch. Assuming nearest neighbor matching, the probability of a mismatch is given by the following equation :

$$\text{Probability of mismatch} = 1 - e^{-(\pi \cdot h^2 \cdot d)} \quad (1)$$

where  $d$  is the density of the noise in dots/deg<sup>2</sup> and  $h$  is the step size in degrees (Ullman, 1979; Williams and Sekuler, 1984). The mean number of dots in a circular area of radius equal to the step size is  $(\pi \cdot h^2 \cdot d)$ , which is equivalent to the mean number of noise dots being closer to the position of the signal dot in frame  $n$  than the signal dot itself in frame  $n + 1$ . If this number is sufficiently small, then the probability that no noise dot causes a mismatch follows a Poisson distribution and thus equals  $e^{-(\pi \cdot h^2 \cdot d)}$ .

When the detection data were plotted as a function of the probability of mismatch, all the curves for the different step sizes were superimposed (lower half of Figure 2). Does this result mean that the human motion system is actually solving the motion correspondence problem based on nearest neighbor matching? Not necessarily. Rather, the superimposed data in the lower half of Figure 2 may mean that the process that limits detection is automatically scaled with step size. The step sizes of the signal and noise dots were kept the same in order to obscure the motion of the signal dot, so our displays were self-similar. Instead of varying step size and density, we could have achieved the same results by increasing the viewing distance from the display. As our next result will show, mismatching, based strictly on nearest neighbor matching, is not the factor limiting signal detection.

## 2) Trajectory detection depends motion cues, not position cues

Since the trajectory motion traced out a straight string of dots over time, it was possible that observers were detecting the signal on the basis of dot collinearity, i.e., on the basis of a position or form cue rather than on a motion cue (Uttal, Brunnell and Corwin, 1970; Falzett and Lappin, 1983). To test whether this was the case, we altered the directional characteristics of noise. Rather than choosing the directions of the noise vectors from all 360 degrees, we narrowed the range to 180 degrees centered on the rightward direction. This change made the noise appear to flow globally towards the right (Williams and Sekuler, 1984). As before, the signal dot was moved in one of eight directions chosen at random, but for this experiment, we scored the percentage correct as a function of the direction of the signal dot. Figure 3 shows that detection depends strongly on the direction of the signal dot relative to the directional range of the noise. When the signal dot moves to the left, it is almost perfectly detected, but when it moves to the right, in the mean direction of the noise, it is much harder to detect. If observers are detecting the signal dot on the basis of a position or form cue, detection should not depend on the mean direction of the random motion noise; only a motion signal would be affected in the manner shown in Figure 3. These results argue that signal detection depends on a motion unit responsive only to a small range of directions. Note further that probability of mismatch, which depends only on step size and density, is the same whether the signal dot moves left or right, so mismatching, based on nearest neighbor matching, does not explain detection in this experiment. The dependence on probability of mismatch shown in Figure 2 implies that the effect of the noise scales with step size, while the results in Figure 3 show that only noise in the direction of the trajectory signal affects detection.

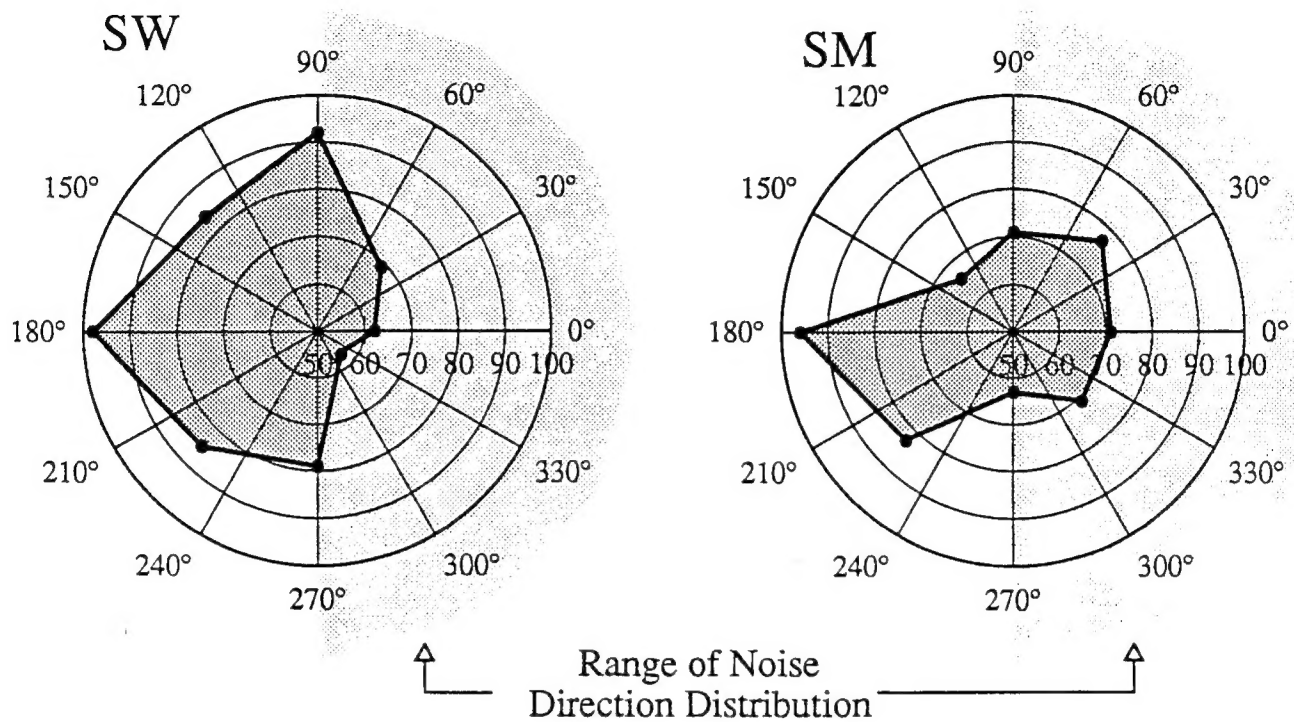


Figure 3

3) *Detection is not limited by the response of single independent motion detectors*

One explanation for our results is that the size of a directionally-sensitive motion detector responding to the trajectory scales with step size. Since the frame rate was the same for all our displays, the speed of both the signal and noise dots increased systematically with step size. Motion units responsive to different speeds could have different-sized receptive fields. The temporal integration time associated with primary motion detectors is roughly 100 msec (Mikami, Newsome & Wurtz, 1986; Burr, 1981; Watson and Nachmias, 1977). If all motion detectors have about the same integration time, then slow speeds (or small step sizes) are detected by motion units with small receptive fields, and fast speeds (or large step sizes) by units with large receptive fields (McKee and Nakayama, 1984). As shown by the diagram in Figure 4, the interaction between step size and density, i.e., "probability of mismatch", is predictable by assuming that the receptive field of the motion detector scales with step size. If detection is limited by the quantity of noise falling within a single motion detector, then increasing the noise density for small step sizes guarantees that the same amount of noise falls within small receptive fields responding to small step sizes as within larger field sizes responding to the larger step sizes. Of course, only the noise vectors that stimulate the preferred direction of the unit responding to the trajectory will affect detection, but the quantity of directional noise will also remain constant if the field size of the motion detector is

scaled with step size.

Our next experiment showed that this scaled-receptive-field explanation, however attractive, was not sufficient to account for trajectory detection. The signal trajectory did not have to be straight to be easily detected. We had measured the tolerance for slow changes in direction from frame-to-frame. Provided the change in direction was small ( $<45^\circ$ ), detection was fairly high (75% correct) for signal dots presented in dense noise. This result suggested that circular trajectories would also be quite visible, and indeed, we found that a circular trajectory was about as detectable as a straight one. Note what happens to the signal falling within a single motion unit if the trajectory is slowly changing direction each frame (24 degree shift in direction each frame). By

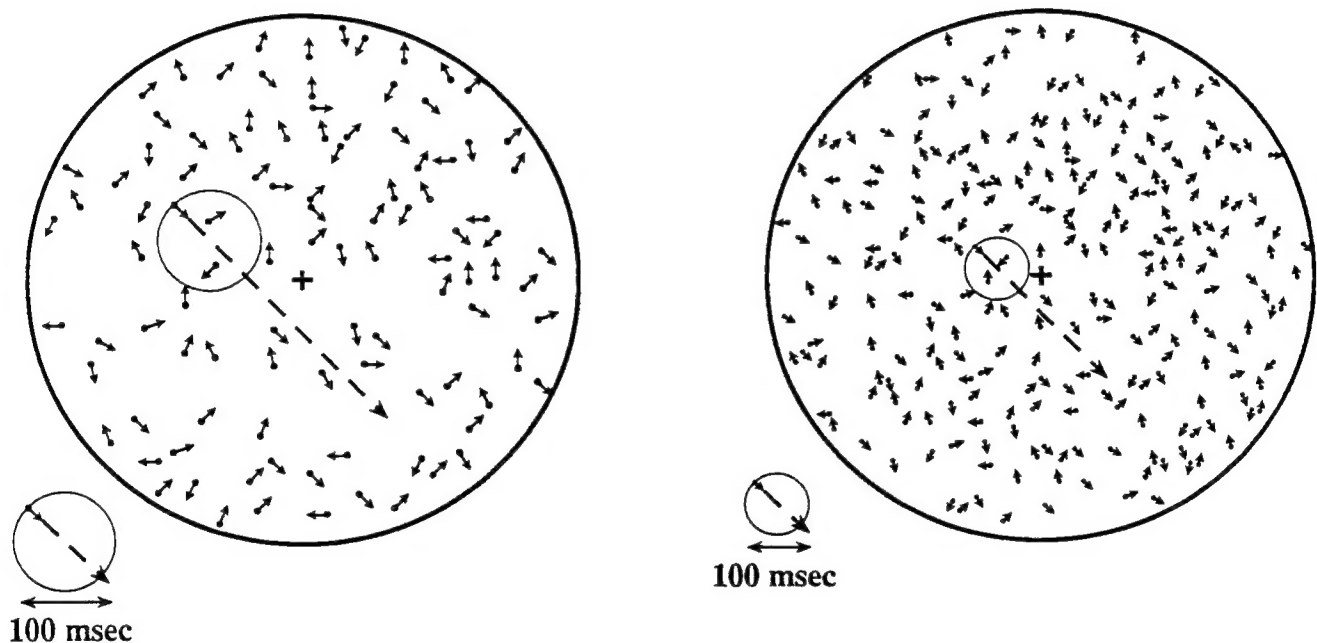


Figure 4

the end of five frames (100 msec), the trajectory is moving orthogonal to its initial direction (see Figure 5). Obviously, this is not a good signal for a unit tuned to the initial direction. Nor is it a particularly good signal for a unit tuned to an oblique direction, one that might respond to the chord of the arc formed by the circular trajectory (the first and fifth dots of the sequence) since such units



would see less of the signal. Yet human performance is the same for the circular and straight trajectories. This result argues for some mechanism that joins signals from adjacent units with similar directional tuning.

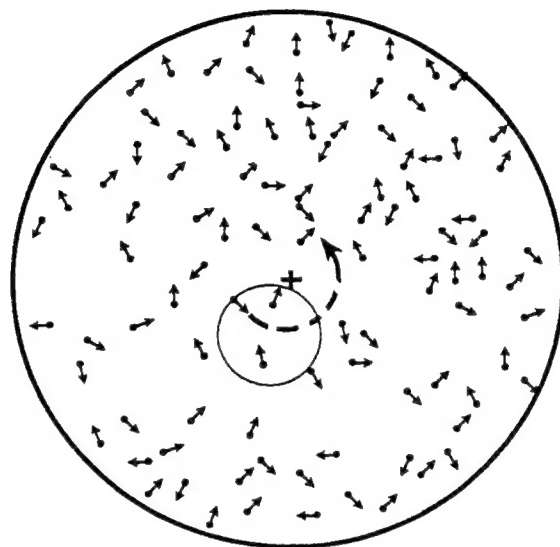


Figure 5

Even more powerful evidence against this single-motion-unit hypothesis comes from consideration of the noise falling within each putative motion unit. Although the noise filling the screen is impressive, the noise associated with each motion unit is very small. For example, if the diameter of the responding motion unit corresponds to the distance moved by the trajectory in five frames (four hops), then, for a step size of  $0.16^\circ$ , the receptive field has an area of  $0.32 \text{ deg}^2$ . At a noise density of  $3 \text{ dots/deg}^2$ , about 1 noise dot falls in this unit every frame, or 5 noise dots in 100 msec -- the same number as the signal. The signal-to-noise ratio is even higher than this value of 1, since most of the motion vectors specified by the noise dots are apt to be orthogonal or opposite to the preferred direction of the unit. Therefore, considering that Newsome, Britten and Movshon (1989) reported that a correlated directional signal of 10% is detectable in noise both by human observers and single units in MT, a single-motion-unit hypothesis would predict almost no effect of noise on performance. But, as shown in Figure 2, this amount of noise does greatly degrade detection.

To make this argument more quantitative, Grzywacz, Watamaniuk and McKee (see

enclosed paper) simulated the response of Gabor motion energy units to 6 frames (120 msec) of a signal dot moving on a straight trajectory through random-motion noise. Figure 6 plots a  $\chi^2$  estimate of the relative response of these units to targets moving in their preferred and null directions<sup>2</sup>:

$$\chi^2 = \frac{R_p - R_n}{|R_p - R_n|} \frac{(R_p - R_n)^2}{R_p + R_n}, \quad (2)$$

where  $R_p$  and  $R_n$  are preferred and null responses respectively, the second fraction is a  $\chi^2$  measure around the mean,  $(R_p + R_n)/2$ , and the first fraction gives the sign of  $R_p - R_n$ . The response is plotted as a function of the receptive field radius<sup>3</sup> in units of step size. For units with larger receptive fields, directional selectivity is close to zero due to the effect of the noise. The best signal is found at a receptive field radius of 2.3 steps, or the diameter traversed in about 5 frames.

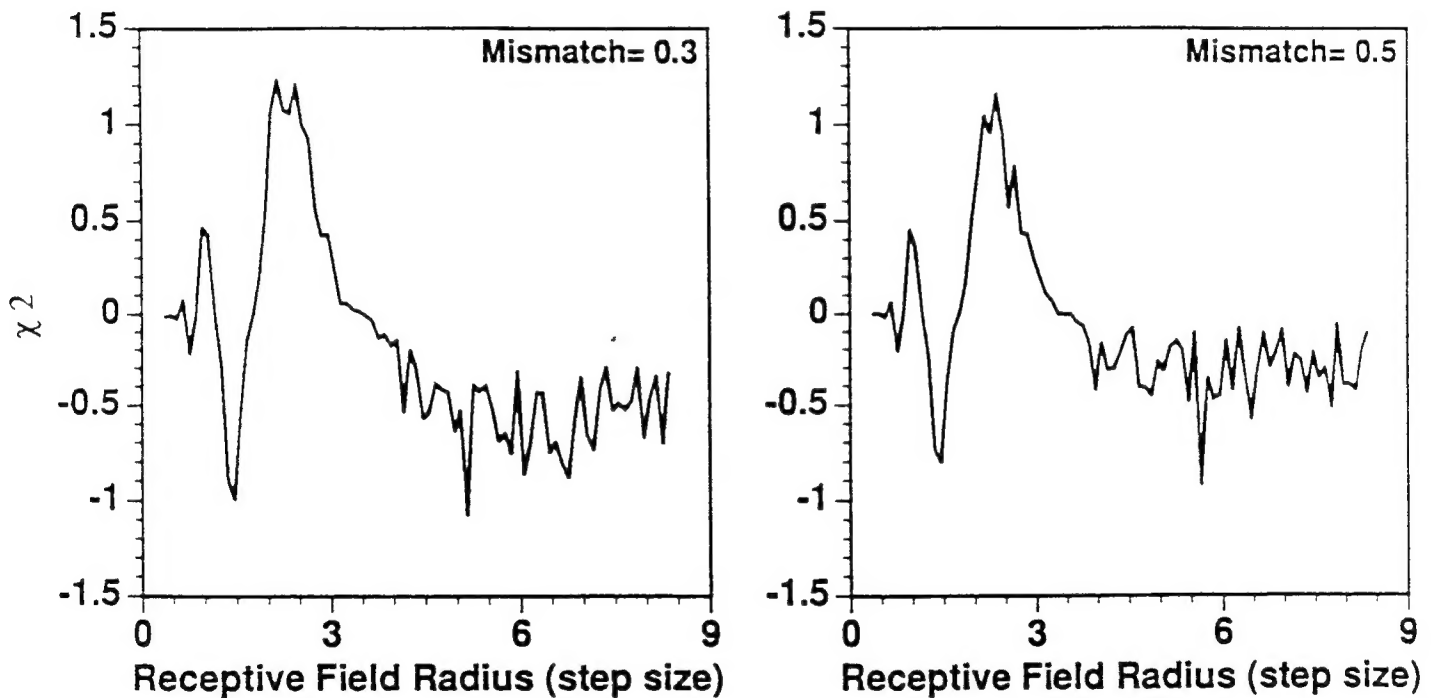


Figure 6

<sup>2</sup> This statistic was used rather than the simple ratio of preferred to null responses because  $\chi^2$  is sensitive to absolute response amplitude, and therefore captures the statistical significance of the ratio.

<sup>3</sup> As given by the standard deviations of the Gaussian envelopes of the Gabor filters used for the simulations.



A secondary positive peak is found at a radius equal to the step size. The negative response at a radius of 1.5 steps indicates aliasing, i.e., the motion unit responds more vigorously to a signal in the null direction than to one in the preferred direction. The two adjacent graphs show simulations for two different probabilities of mismatch (0.3 and 0.5), which, for any given step size, correspond to two different noise densities. Note that the magnitude of the peak response is barely affected by increasing the noise density, although human detection is near chance for a probability of mismatch of 0.5. So, if human motion units resemble the units in the motion energy model, noise in single independent motion units cannot account for our results.

If we were to place a small circular aperture on the screen so that five frames of the trajectory moved through the aperture on every trial, the observer would always detect the signal, unless the noise was so dense that it virtually filled the aperture. Why is the signal dot so difficult to detect in the sparse noise of our much larger displays? One possibility is that the observer is engaged in some type of search task, and that the signals produced by the noise act as "distractors" (Treisman and Gelade, 1980). The observer is forced to go through every small area in the display looking for a motion signal that is significantly larger than the signals produced by the noise. A higher noise density means more distractors, so if the stimulus duration is short, the observer does not have time to find the signal, and gets only a small percentage correct. Of course, the trajectory signal does not remain conveniently in a single location, but, for some search strategies, there could be as much chance of encountering a moving signal as of finding a five-frame signal presented repeatedly in one place.

In this view, there is nothing special about the motion trajectory, so no special network is required to detect it. The trajectory is just an efficient way of increasing the signal in several local motion detectors above the signals produced by the distracter dots in other units. For example, if five frames of sampled motion (100 msec) are the number detected by the receptive field of a local motion unit, then a straight trajectory of 10 frames produces six sequences of five frames each. If the observer is searching for any unit with a strong motion signal, he or she has a high chance of finding at least one of these six units. This view cannot be correct because we have shown that the extended sequential arrangement of trajectory motion is important to detection. In one experiment, we distributed, throughout the noise, six five-frame segments equivalent to the number of segments that form a ten-frame straight trajectory; the trajectory was more easily detected than the distributed components. Also, our results with the circular trajectory show that detection is relatively easy when none of the local motion units have a signal that is much stronger than the signals produced by the motion of the noise.

The observed superiority of the trajectory is not the only problem with a simple search explanation. Why does success in finding the trajectory dot depend on probability of mismatch? Why is the trajectory dot always visible in the midst of a hundred noise dots under some conditions (small step sizes), but completely hidden in others (large step sizes)? To account for this finding, the search area would have to scale inversely with speed. Some process would have to reduce the size of the search area to a small region when the speed is very slow, and increase it to include the whole field when the speed is very fast, thereby keeping the effective number of "distractors" constant. It has been suggested that the size of the window of attention automatically scales with the size or scale of the searched-for object (Sperling and Melcher, 1978; Nakayama, 1990), but, to our knowledge, no one has suggested an automatic scaling with speed.

Cognitive processes such as selective attention undoubtedly define the region over which the brain searches for the signal, but our data suggest that the effects of noise on detection are

mediated by the human motion system (Figure 3). Since the noise does not affect the primary motion units directly, we think that the constraints on signal detection are set by neural operations that occur in the motion system *after* initial processing by the primary motion detectors. These operations, in turn, make it difficult to find a motion unit with a signal greater than that produced by the noise, no matter what search strategy is adopted by the brain. We next describe a computational model of these operations and show that it simulates our experimental results quantitatively.

## B. Computational Results

The velocity of a moving object, i.e., any visible feature with contours at various orientations, cannot typically be specified by a single motion detector, since each detector responds preferentially to that component of the motion perpendicular to its preferred orientation. Signals from motion units, responding differentially to the various object contours, must be combined in some fashion to obtain a single coherent estimate of object velocity. Motion coherence has received considerable attention in the context of plaid motion (Adelson and Movshon, 1982; Welch, 1989; Ferrera and Wilson, 1990; Wilson, 1991). Operations that account for the coherence of plaid motion must, of course, also apply to any local field of image velocity vectors. Yuille and Grzywacz (1988; 1989) proposed a general computational theory that smoothed the velocity field by minimizing a cost function; they showed that this theory, which they called "Motion Coherence", produced a coherent estimate of object motion and could account for a number of psychophysical results. Grzywacz, Smith and Yuille (1989) extended the model to enforce consistency over time as well as over space ("temporal coherence").

The current version of this theory is described fully in the accompanying paper (Grzywacz, Watamaniuk, and McKee). Briefly, it consists of three hierarchical stages. The first, which we call the Local stage, estimates motion in localized regions of a multi-dimensional space whose independent variables are space, time, direction of motion, speed and spatial scale (or spatial frequency). We think of the motion measurements at this stage as being generated by primary motion detectors -- units tuned to particular values of all these variables, except for time. The second stage, the Coherence stage, smooths these local measurements within neighborhoods in this multi-dimensional space. Consequently, this stage transforms the local multi-dimensional space into a new multi-dimensional space defined by the same independent variables. The final stage, which we call the Outlier stage, implements a decision rule, so that the results of the computer simulations can be compared to human psychophysics. It simulates a search within a large region of the space defined by the motion measurements, but confined to a fairly narrow range of directions. Using an approximation to the Dixon statistic often used to remove outliers (Dunn and Clark, 1987), the computer determines if there is a signal in each directional bandwidth which is sufficiently larger than the rest of the measurements to be considered an outlier, and identifies this outlier as the signal dot.

Since the Coherence stage is the most important for explaining our results, we will describe it in some detail. Conceptually, there are three components to the stage. One component, which we call neighborhood coherence, accounts for the influence of the surrounding noise on the detection of the signal dot. At any instant of time, this component enforces consistency over a neighborhood within the multi-dimensional space; in particular, it minimizes differences between local units within a small spatial region whose size increases proportionally to the spatial scale of the local units. In our computer implementation, smoothing is only enforced between adjacent

neighbors tuned to the same spatial scale and to similar directions (bandwidth = 45 deg). Consider what happens if a noise dot happens to stimulate a similar unit adjacent to the unit responding to the trajectory. In minimizing the difference between the two units, the smoothing operation reduces the signal from the unit responding to the trajectory to near the same level as the unit responding to the noise dot. As the noise density is increased, the chance that a neighboring unit will be stimulated by a noise dot increases, producing a frequent reduction in the response to the signal dot as it moves along its trajectory. At very high densities, the response to the signal dot is seldom higher than the response to various noise dots within the display, so the trajectory dot fails to meet the statistical criterion of the Outlier stage. As shown in Figure 6, the response of the local units to the signal dot scales with step size, being maximal for a unit with a radius 2.3 times the step size. In the implementation of the model, to enforce the proportionality between the spatial scale of the local-motion units and the size of neighborhood for coherence, the smoothing operation was enforced only between adjacent units of the same spatial scale. Hence, as the step size got larger, the optimal scale detecting the signal dot increased, and the spatial region associated with neighborhood coherence increased proportionally. This property explains why detection was limited by probability of mismatch (Figure 2).

What accounts for the high detection rate in moderately dense noise? The countervailing force is the "temporal coherence" component which reinforces directional consistency over time. Since only the trajectory dot moves in a consistent direction, the signals of units responding to the trajectory are enhanced relative to signals generated by the noise. The immediate past information from units in the Coherence stage is compared to present information. Activity in a directionally-selective unit implies a direction from which the signal could have come; the temporal coherence component checks whether there was the same or a similar directional signal at a position corresponding to the implicit location of the motion signal in the immediate past. In the implementation used to model our psychophysical results, only neighboring units at the same scale and similar directional bandwidth were compared. Finally, although both the neighborhood and temporal coherence components smooth responses from the primary motion units, the coherence measurements are still constrained to agree with the measurements from the Local stage, so a third component minimizes differences between the Coherence units and the primary motion units of the Local stage.

A mathematical representation of the Coherence stage would find the  $R_c$  that minimizes the following energy function:

$$\begin{aligned}
 E(t) = & \sum_{\vec{r}, \vec{u}, s, \lambda} (R(t: \vec{r}, \vec{u}, s, \lambda) - R_c(t: \vec{r}, \vec{u}, s, \lambda))^2 \\
 & + \int_{\vec{r}, \vec{u}, s, \lambda} \varphi_r (D_r R_c)^2 + \varphi_u (D_u R_c)^2 + \varphi_s (D_s R_c)^2 + \varphi_\lambda (D_\lambda R_c)^2 \\
 & + \int_{\vec{r}, \vec{u}, s, \lambda} \varphi_t \int_{s'} W(s') \left( \frac{\partial R_c}{\partial t} - s' \nabla_r R_c \cdot \vec{u} \right)^2
 \end{aligned} \tag{3}$$

The directionally selective cells in both the Local and Coherence stages can be characterized by the middle of the receptive fields ( $\vec{r}$ ), the preferred direction of motion ( $\vec{u}$ ), preferred speed ( $s$ ), and spatial scale or receptive field size ( $\lambda$ ). The activity of one such cell in the Local stage can be

written as  $R_l(t: \vec{r}, \vec{u}, s, \lambda)$ , where  $t$  is time and the quantities following the colon are parameters of the cell. Similarly, the activity of the corresponding cell in the Coherence stage can be written as  $R_c(t: \vec{r}, \vec{u}, s, \lambda)$ . The first term of equation (3) imposes consistency with the local measurements from the primary motion units, since it minimizes the differences between  $R_c$  and  $R_l$ . The second term smooths the responses across neighborhoods, by reducing the magnitudes of differentiations of  $R_c$ . These  $D_x$  operators would normally be partial derivatives, gradients or more general operators using a combination of derivatives of various orders (Yuille and Grzywacz, 1989). However, these operators are also functions of the local data, and are constrained in two important ways. First, if the local data ( $R_l$ ) change too quickly in any direction in the multi-dimensional space, then data around that point are not used in the derivative estimate. Secondly, the spatial operator is a function of  $\lambda$ , that is,  $D_r = D_r(\lambda, R_l)$ .

This constrains the size of the spatial neighborhood to be proportional to its spatial scale. One way to implement this requirement is to keep the inter-neighbor spatial distance proportional to  $\lambda$  and to estimate derivatives from neighbor responses. Another way is to define  $D_r$  as an operator using a combination of derivatives of various orders, which implements smoothing with a Gaussian approximation, whose standard deviation can be made proportional to  $\lambda$  (Yuille and Grzywacz, 1989).

The bottom integrals impose temporal coherence by using an integrand that is reminiscent of the "image constraint equation" of Fennema and Thompson (1979) and Horn and Schunck (1981). The main difference between their formulation and that in Equation 3 is that the new equation uses spatio-temporal derivatives of the response instead of brightness. In a sense, this equation measures the movement of the local response, rather than the movement of the image. The other difference is that Equation 3 eliminates speed ( $s'$ ) dependence through integration with the weight (probability density) function  $W(s')$ . To obtain the bottom integrand (except for  $W$ ), one postulates that there is a minimal difference between the responses of a cell "A" with particular preferred direction and the past responses of other cells with the same preferred direction and whose receptive fields are located in positions for which the preferred direction point to the receptive field of "A". Mathematically, this difference can be approximated as:

$$R_c(t: \vec{r}, \vec{u}, s, \lambda) - R_c(t - \Delta t: \vec{r} - s' \Delta t \vec{u}, \vec{u}, s, \lambda) \approx \frac{\partial R_c}{\partial t} - s' \nabla_r R_c \cdot \vec{u} \quad (4)$$

To test whether this computational model could reproduce our results, we used a simplified implementation to simulate the conditions of our experiments (see enclosed paper for details of the computational methods). Two parameters, the value of the detection threshold for the Outlier stage and the standard deviation of an internal noise, were estimated from the subjects' performance in one standard experimental condition -- a straight 260 msec trajectory signal presented at a probability of mismatch of 0.3.

Two results from this simulation are described next. First, it was shown that the computer simulation could mimic the decline in performance with increasing probability of mismatch for a wide range of step sizes. The straight line in Figure 7 shows the predicted performance from the computer simulation; data from the subjects are shown for comparison. The model predictions are in good agreement with human performance except at very low mismatch probabilities. As a

second challenge, we simulated the response of the model when the directions of the vectors in the random motion noise were confined to a bandwidth of 180 degrees (see Figure 3 above). Qualitatively, the simulation, shown by the solid and dashed lines in Figure 8 below, resembles the performance of the subject. The only significant discrepancy was the higher sensitivity of the model when the difference between the direction of the signal and the mean direction of the noise is around 135 deg.

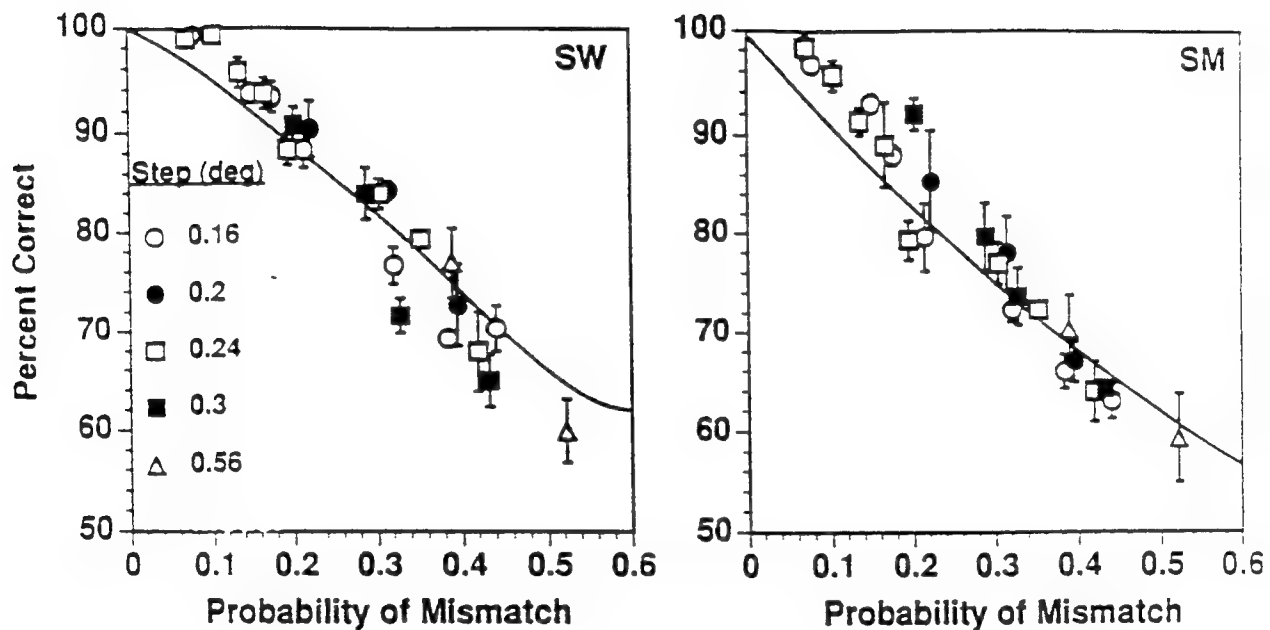


Figure 7

For computational simplicity, the local motion units that provided the input to the coherence stage were very crude. They responded equally to any signal falling within a 45 deg bandwidth, but gave no response outside this range. This sharp tuning, which is improbable biologically, may account for the discrepancy.

In addition, the model, as implemented, does simulate human performance with circular trajectories. Sequential activity in adjacent motion units tuned to the same or similar directions is enhanced by temporal coherence relative to the signals generated by the noise. The model predictions show the same improvement in performance with increasing duration as that exhibited

by the human observers.

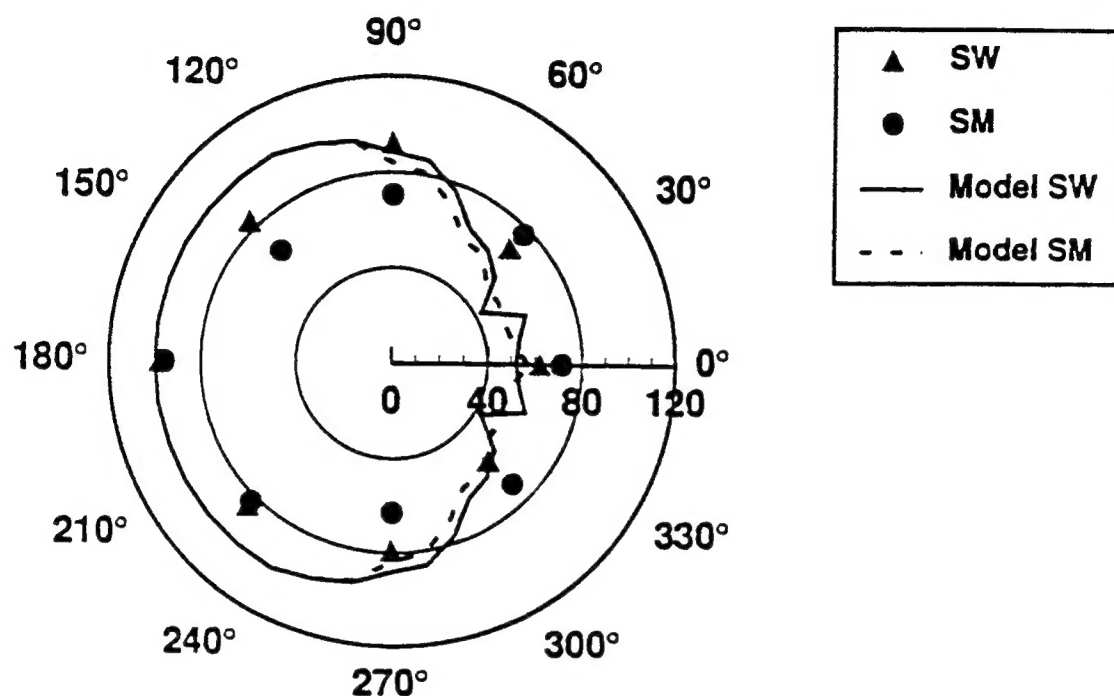


Figure 8

## II. OTHER PROJECTS

### A. Motion Transparency

Motion transparency challenges some contemporary motion models, because the visual system appears to assign two different directions and/or speeds to the same location. Most experimental studies of motion transparency have used the familiar plaid pattern, composed of two superimposed drifting gratings presented at different orientations. In some conditions, the drifting gratings cohere into a rigid structure moving in a single direction, while in others, the gratings appear to slide across one another ("transparency"). Sparse random dot patterns have also been used to create the appearance of transparent surfaces that glide past each other in opposite directions (Ullman, 1984; Treue, Husain and Anderson, 1991).

Bravo and Watamaniuk (see enclosed paper) used a sparse random dot cinematogram to study the motion transparency produced by differences in speed. In their display, all dots moved in the same direction at one of two speeds. Two transparent surfaces were seen provided that 1) the difference between the two speeds was substantial (at least a factor of two), and 2) that dots moving at each of the two speeds were presented *simultaneously*. Rapid synchronous alternation



(every 20 - 40 msec) between the two speeds did not produce transparency. When this segmentation into transparent surfaces occurred, observers could discriminate the speed of the dots associated with one surface without any interference from the dots moving on the other surface. Bravo and Watamaniuk showed that the initial segmentation into two surfaces was based on a very imprecise speed signal. After segmentation, the visual system integrated across each of the two transparent surfaces to improve the precision of the speed signal. The Smith-Grzywacz transparency model can account for the initial segmentation based on speed, and probably for the subsequent integration of signals within planes. The Nowlan-Sejnowski model (Nowlan and Sejnowski, 1993) may also be able to account for these results.

To summarize, the results from the study by Bravo and Watamaniuk suggest that 1) the motion system calculates local velocities; 2) it determines whether there is a single candidate velocity or several "winners"; 3) it segments the visual field into planes based on the number of local velocities; 4) then it integrates across the planes specified by the local velocities to improve the precision of the speed signal.

### B. Motion-in-Depth

Objects that move in depth toward or away from the observer's eyes produce image motions on the two retinae that differ in speed or direction or both. As Regan (1993) noted in a recent short communication in *Vision Research*, there are two alternative ways to encode motion-in-depth. The brain may use the difference (ratio) of the two monocular velocities (Beverley and Regan 1973; 1975) or the change in disparity over time. Cumming and Parker (1994) created a stereoscopic stimulus that had no correlated motion in either of the monocular half-images. They manipulated the disparity of the stimulus over time so that the stimulus appeared to be moving in depth. The smallest detectable motion-in-depth threshold was equal or better than similar thresholds measured with stimuli containing correlated motion in the half-images. Cumming and Parker concluded that there was no neural mechanism sensitive to inter-ocular velocity differences; motion-in-depth was mediated by changes in disparity over time. However, subjects in this study were not required to make a pure motion judgment, so they may have been disparity cues alone. Harris and Watamaniuk (see enclosed paper) used the Cumming and Parker stimulus (no monocularly-correlated motion) to measure speed discrimination for targets moving in depth. Although this target appeared to move in depth, their subjects were unable to judge target speed. Subjects could judge the motion-in-depth speed precisely only when the monocular half-images contained motion information. A series of experimental manipulations revealed that subjects had to compare the speeds of the two half-images in order to make this judgment. Thus, there must be a neural mechanism that compares inter-ocular velocity differences.

### C. Detecting a Trajectory in Three-Dimensional Noise

One function of stereopsis is to break camouflage. Is a trajectory moving in 3-D through three-dimensional noise more easily detected than a 2D trajectory presented in two-dimensional noise (our standard condition)? We measured detection of trajectory motion as a function of the number of noise dots filling a cylindrical space viewed stereoscopically. We compared 3D detection of the trajectory to a 2D control condition in which the subjects viewed one of the half-images of the stereogram binocularly. There was a consistent improvement in detection in the 3D condition, but it was surprisingly small -- about 25% at best. We concluded that the neural representation of three-dimensional space is not isotropic. Human resolution of the third-



dimension is very coarse, so detection of features embedded in three-dimensional noise is not aided much by stereopsis. A manuscript describing these results is in preparation.

## VI. PUBLICATIONS SUPPORTED BY GRANT

### Papers

- Watamaniuk, S.N.J. (1992) Visual persistence is reduced by fixed-trajectory motion, but not by random motion. *Perception*, 21, 791-802
- Watamaniuk, S.N.J. and Duchon, A. (1992) The human visual system averages speed information. *Vision Research*, 32, 931-942.
- McKee, S.P. and Welch, L. (1992) The precision of size constancy *Vision Research*, 32, 1447-1460.
- Watamaniuk, S. N. J., Grzywacz, N. M. & Yuille, A. L. (1993). Dependence of speed and direction perception on cinematogram dot density. *Vision Research*, 33, 849-859.
- Bravo, M. J. & Watamaniuk, S. N. J. (1995). Evidence for two speed signals: a coarse local signal for segregation and a precise global signal for discrimination. *Vision Research*, In Press.
- Watamaniuk, S.N.J., McKee, S.P. and Grzywacz, N. (1995) Detecting a trajectory embedded in random-direction motion noise. *Vision Research*, 65-78.
- Vaina, L.M., Grzywacz, N.M., and Kikinis, R. (1994). Segregation of computations underlying perception of motion discontinuity and coherence. *NeuroReports*, In Press.
- Harris, J.M. and Watamaniuk, S.N.J. (1995) Speed discrimination of motion-in-depth using binocular cues. *Vision Research*, In Press.
- Grzywacz, N.M., Watamaniuk, S.N.J. and McKee, S.P. (1995) Temporal coherence theory for the detection and measurement of visual motion. *Vision Research*, In Press.
- Watamaniuk, S.N.J. and McKee, S.P. (1995) Seeing motion behind occluders. Submitted to *Nature*.

### Chapters Supported by Grant

- Vaina, L.M. and Grzywacz, N.M. (1992) Testing computational theories of motion discontinuities: A psychophysical study, in Sandini, G. (Ed.) *Lecture Notes in Computer Science*, 588, Springer-Verlag, Berlin. 212-216.
- Smith, J.A. and Grzywacz, N.M. (1993) A local model for transparent motions based on spatio-temporal filtering, Eeckman, F.H. and Bower, J.M. (Eds.) *Computation and Neural Systems*, Kluwer Academic Press.
- Grzywacz, N.M., Harris, J.M. and Amthor, F.R. (1994) Computational and Neural Constraints for the Measurement of Local Visual Motion. *Visual Detection of Motion*, Smith, A.T. and Snowden, R.J. (Eds.) Academic Press, London, 19-50
- McKee, S.P. and Watamaniuk, S.N.J. (1994) The psychophysics of motion perception. *Visual Detection of Motion*, Smith, A.T. and Snowden, R.J. (Eds.) Academic Press, London. 85-114.

### Abstracts Supported by Grant

- Watamaniuk, S.N.J. (1992) Simultaneous direction information from global flow and a local trajectory component *Investigative Ophthalmology and Visual Science* (Suppl.), 33, 1050.
- Bravo, M.J. and Watamaniuk, S.N.J. (1992) Speed segregation and transparency in random dot displays. *Investigative Ophthalmology and Visual Science* (Suppl.), 33, 1050.
- Grzywacz, N.M. (1992) One-path model for contrast-independent perception of Fourier and non-Fourier motions. *Investigative Ophthalmology and Visual Science* (Suppl.), 33, 954
- Watamaniuk, S.N.J. and Bravo, M.J. (1992) Transparency influences speed discrimination in random dot displays. *American Psychological Society Presentation*, June 1992.
- Watamaniuk, S.N.J., McKee, S.P., and Sekuler, R. (1992) Is luminance a cue for matching in random-dot motion displays? *Optical Society of America Annual Meeting Technical Digest*, 23, 215-216.
- Plant, G. and Watamaniuk, S.N.J. (1993) A failure of motion deblurring in the human visual system. *Investigative Ophthalmology and Visual Sciences* (Suppl.), 34, 1230
- Watamaniuk, S.N.J. and McKee, S.P. (1993) Why is a trajectory more detectable in noise than correlated signal dots? *Investigative Ophthalmology and Visual Sciences* (Suppl.), 34, 1364.
- McKee, S.P., Watamaniuk, S.N.J., Harris, J.M. and Taylor, D.G. (1994) Detecting moving features in 3-dimensional noise. *Investigative Ophthalmology and Visual Sciences* (Suppl.), 35, 1986
- Harris, J.M. and Watamaniuk, S.N.J. (1994) Speed discrimination of binocular motion in depth. *Investigative Ophthalmology and Visual Sciences* (Suppl.), 35, 1986.
- Watamaniuk, S.N.J., McKee, S.P. and Taylor, D.G. (1994) Detecting a trajectory moving behind occluders. *Investigative Ophthalmology and Visual Sciences* (Suppl.), 35, 2162.
- Watamaniuk, S.N.J. and Heinen, S.J. (1994) Smooth pursuit eye movements to dynamic random-dot stimuli. *Society for Neuroscience Abstracts*, 20, 317.
- Harris, J.M. & Watamaniuk, S.N.J. (1994) Speed discrimination of the motion of an object defined only by binocular disparity. *Perception* (Suppl), 23, 60.
- McKee, S.P., Harris, J.M., & Watamaniuk, S.N.J. (1995) Detection of motion-in-depth is disrupted by static disparity. Submitted to the European Conference on Visual Perception.
- Watamaniuk, S.N.J. & Heinen, S.J. (1995) Is the visual system's insensitivity to acceleration also evident in the smooth pursuit system? *Investigative Ophthalmology and Visual Sciences* (Suppl), in press.
- Harris, J.M. & Watamaniuk, S.N.J. (1995) A poor speed signal for disparity defined motion. *Investigative Ophthalmology and Visual Sciences* (Suppl), in press.